Heliyon 10 (2024) e27808

Contents lists available at ScienceDirect

Heliyon

journal homepage: www.cell.com/heliyon

Research article

Combined analysis of bulk RNA and single-cell RNA sequencing to identify pyroptosis-related markers and the role of dendritic cells in chronic obstructive pulmonary disease

Huiyan Zheng, Guifeng Wang, Yunlai Wang, Qixian Wang, Ting Sun *

Department of Health Management Center, The Second Affiliated Hospital of Zhejiang University School of Medicine, Hangzhou, Zhejiang, China

ARTICLE INFO

Keywords:
Chronic obstructive pulmonary disease
Machine learning
Diagnostic model
Biomarkers
Immune infiltration
Dendritic cell

ABSTRACT

Chronic obstructive pulmonary disease (COPD) is characterized by dyspnea caused by airflow limitation. Further development may lead to decreased lung function and other lung diseases. Pyroptosis is a type of programmed cell death that involves multiple pathways. For example, the pathway induced by the NLR family pyrin domain containing 3 (NLRP3) inflammasome is closely associated with COPD exacerbation. Therefore, in this study, various machine learning algorithms were applied to screen for diagnostically relevant pyroptosis-related genes from the GEO dataset, and the results were verified using external datasets. The results showed that deep neural networks and logistic regression algorithms had the highest AUC of 0.91 and 0.74 in the internal and external test sets, respectively. Here, we explored the immune landscape of COPD using diagnosis-related genes. We found that the infiltrating abundance of dendritic cells significantly differed between the COPD and control groups. Finally, the communication patterns of each cell type were explored based on scRNA-seq data. The critical role of significant pathways involved in communication between DCS and other cell populations in the occurrence and progression of COPD was identified.

1. Introduction

Chronic obstructive pulmonary disease (COPD) is a common respiratory disease characterized by reversible airway obstruction and decreased lung function [1,2]. The pathogenesis of COPD is complex and may involve genetic factors, smoking, and airway inflammation [3,4]. Further development will lead to a higher risk of lung cancer than in normal individuals. Early diagnosis and treatment of COPD can effectively improve patient prognosis [5]. Therefore, there is an urgent need to develop biomarkers related to COPD diagnosis and treatment.

Pyroptosis is an important form of programmed cell death. Morphologically, pyroptosis is characterized by cell swelling, membrane rupture, and exudation of cell contents, leading to cell death [6,7]. Therefore, pyroptosis clears pathogens. Many studies have confirmed the critical role of pyroptosis in tumors [8,9]. The role of pyroptosis-related nucleotide-binding domain-like receptor protein 3 (NLRP3) in COPD has been previously confirmed. Wang et al. showed that TREM-1 promotes lung injury and inflammation in COPD mice by activating NLRP3 inflammasome-mediated pyroptosis [10]. Zhang et al. found that phototherapy can improve lung

* Corresponding author. Department of Health Management Center, The Second Affiliated Hospital of Zhejiang University School of Medicine, Hangzhou, Zhejiang, China.
E-mail address: 1195037@zju.edu.cn (T. Sun).

https://doi.org/10.1016/j.heliyon.2024.e27808
Received 30 September 2023; Received in revised form 23 February 2024; Accepted 6 March 2024
Available online 8 March 2024

function by inhibiting signaling pathways such as NLRP3 to reduce inflammation and pyroptosis in COPD rats [11]. The NLRP3 inflammasome is involved in cigarette smoke extract-induced human bronchial epithelial cell damage and pyroptosis, which provides new insights into COPD [12].

To explore the critical role of pyroptosis-related genes in the occurrence and development of COPD, we mined COPD diagnosis-related genes (DRGs) based on a series of bioinformatics methods. Specifically, we gained access to the GEO database (https://www.ncbi.nlm.nih.gov/geo/). Differentially expressed genes (DEGs) were identified by differential analysis and intercrossed with pyroptosis-related genes (PRGs) reported in the literature to obtain pyroptosis-related differentially expressed genes (PDEGs). Next, we determined the DRGs associated with COPD using different machine-learning algorithms. Subsequently, a diagnostic model for COPD was constructed and validated using an external dataset. We explored the immune landscape of DRGs and their susceptibility to various drugs. As the abundance of infiltrating dendritic cells (DC) differed significantly between the disease and control groups, we identified significant communication pathways between the DC population and other cell populations based on scRNA-seq data.

2. Method

2.1. Data collection and download

In this study, transcriptome data of COPD and control samples were downloaded from the GEO database. We used GSE76925 (40 control and 111 COPD samples) as the training set and GSE47460 (91 control and 145 COPD samples) as the test set. scRNA-seq data for COPD were obtained from the GSE227691 dataset. These included four control, four mild COPD, and four moderate COPD samples.

2.2. Screening of DEGs

For consolidated data, the limma algorithm [13] was used to analyze differentially expressed data, $|\log FC|>0$, and $p < 0.05$.

2.3. Analysis of enrichment

KEGG enrichment analysis and Metascape analysis were performed for DEGs, respectively. Specifically, the KEGG enrichment analysis of the R package "clusterProfiler" [14] obtained significant pathways involved in multiple DEGs ($p < 0.05$). In addition, we used the online Metascape website (https://metascape.org/gp/index.html) to analyze DEGs further.

2.4. Screening of diagnosis-related genes by machine learning algorithm

The scikit-learn package [15] was used to implement the machine-learning models. First, the random forest (RF) algorithm was used to obtain the weights of the intersecting genes. The intersecting genes were ranked by weight. For the ranked genes, logistic regression (LR), support vector machine (SVM), RF, and deep neural network (DNN) were used to select the top-ranked genes individually to construct a model, and the AUC corresponding to the number of different features was recorded.

For the parameter Settings that RF assigns weights to genes: 'n_estimators' set values ranging from 500 to 1000 with a step size of 100. The 'criterion' was chosen between 'gini' and 'entropy.' For the LR algorithm: 'C' values ranged from 0.1 to 2 with a step size of 0.5. For the SVM algorithm, 'kernel' was selected in the 'linear,' 'poly,' 'rbf' and 'sigmoid.' The value of 'degree' ranged from 1 to 2 with a step size of 1. For the DNN algorithm: 'solver' was selected in 'lbfgs,' 'Adam,' and 'SGD.'

2.5. Construction of the nomogram model

For DRGs, we used a nomogram to predict COPD. Specifically, the R package "rms" was used to construct a nomogram for DRGs, and calibration curves were used to evaluate the performance of the nomogram model. In addition, the clinical usefulness of the nomogram was assessed using curve analysis (DCA).

2.6. The immune landscape of DRGs

To determine the relationship between DRGs and immune cells, we applied the CIBERSORT algorithm [16] to evaluate the abundance of 22 immune cell infiltrates in the COPD samples. Additionally, we explored the correlation between DRGs and immune cells using the Spearman correlation analysis.

2.7. Analysis of DRGs and drug interactions

The drug-gene interaction database DGIdb (https://www.dgidb.org) was used to identify potential therapeutic drugs for COPD. Specifically, we uploaded DRGs to the DGIdb database and identified potential drugs and molecular compounds that may be related to DRGs.

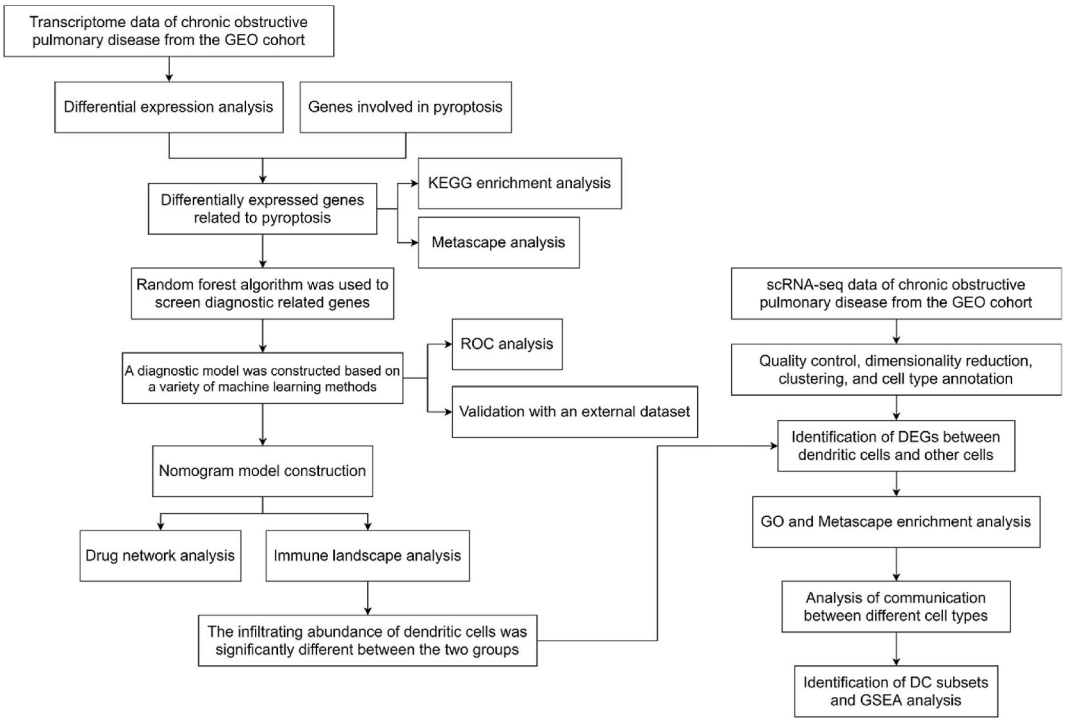

Fig. 1. Overall flow chart of the paper.

2.8. Processing and analysis of scRNA-seq data

In this study, raw scRNA-seq data quality control was performed based on the R package "Seurat" [17]. Specifically, in this study, in addition to the mitochondrial content greater than 20%, red blood cell-related genes (HBA1, HBA2, HBB, HBD, HBE1, HBG1, HBG2, HBM, HBQ1, and HBZ) greater than 5%, the nFeature_RNA selection is less than or greater than 200 to 7500, and nFeature_RNA greater than 1 to 100,000 cells. Finally, cells that met the quality control conditions were retained. After normalization, principal component analysis (PCA) was performed on the top 2000 highly variable genes. Clusters were identified at a resolution of 0.8 based on the first 20 principal components. Cluster-specific tags were identified using the R package " SingleR " [18]. The FindAllMarkers function based on the "Seurat" package identified DEGs for different types of cell populations. Metascape and GO enrichment analyses were performed on the DEGs in the dendritic cell population. Metascape analysis results were obtained from the Metascape database (https://metascape.org/gp/index.html#/main/step1). Communication between various cell populations was inferred using the R package 'CellChat' [19]. The software package calculates the communication network (number and strength) between different cell populations by counting the links and collecting the communication probabilities.

3. Results

3.1. Acquisition and enrichment analysis of DEGs related to pyroptosis

An overall flowchart of this study is shown in Fig. 1. First, we performed differential expression analysis of transcriptome data from the GSE76925 dataset. Fig. 2A and B presents the heat and volcano maps obtained during the differential expression analysis. The heatmap shows that the expression of DEGs in the diseased and control groups was significantly different. Finally, 8219 DEGs were identified. We obtained 110 PRGs from the literature and then intersected them with the DEGs. Finally, 35 intersecting genes were identified (Fig. 2C). As shown in Fig. 2D, the expression of 35 genes differed significantly between the two groups. Finally, we present the results of KEGG enrichment analysis and Metascape enrichment analysis for the intersecting genes in Fig. 3A and B, respectively. In Section IV, we discuss the vital role of these pathways in the development and progression of COPD in detail.

3.2. Construction and validation of diagnostic models

To screen genes related to COPD diagnosis, this study first assigned weights to intersecting genes based on RF, with higher weights representing higher diagnostic importance of genes. The mean weight of 0.0344 g was calculated for these genes—fourteen genes with weights greater than the mean were retained. The corresponding weighted bar plots for these genes are shown in Fig. 4A. The ROC curves of the diagnostic models constructed using all algorithms in the internal and external datasets are shown in Tables 1 and 2,

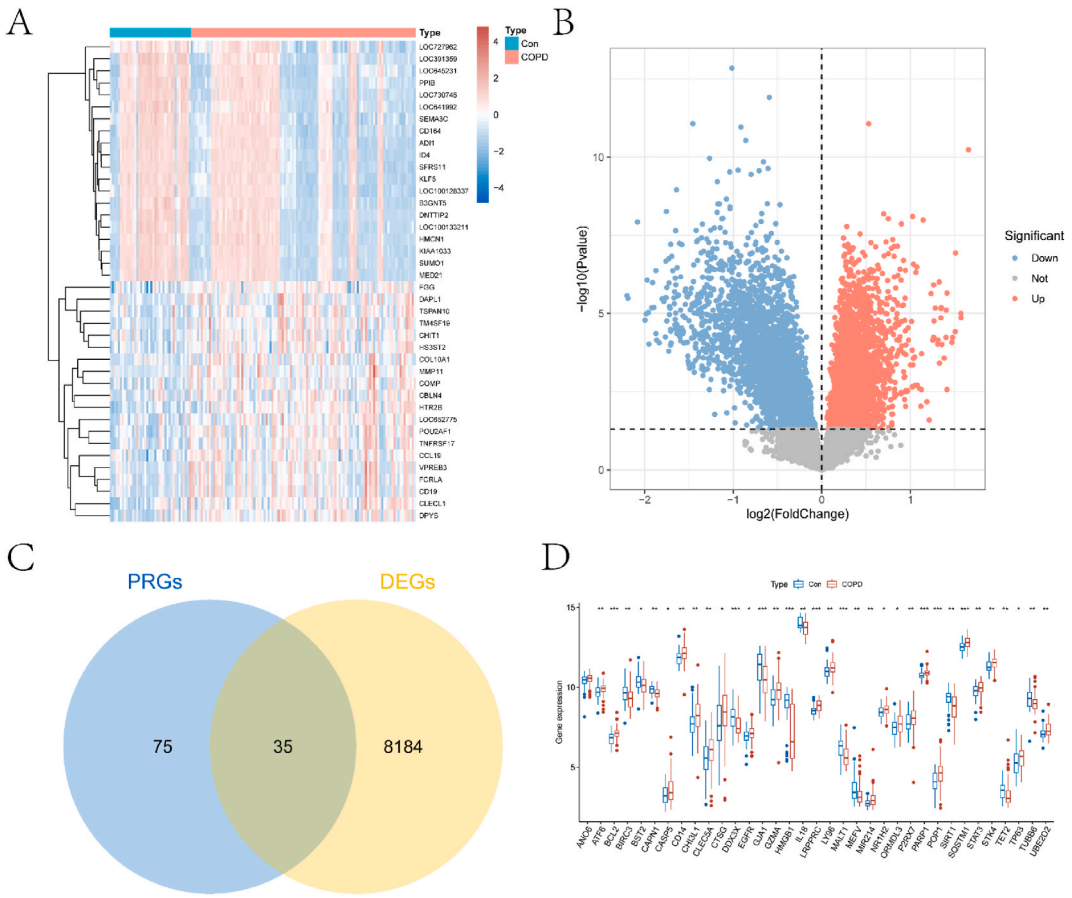

Fig. 2. Results of differential expression analysis and the intersection of PRGs and DEGs. A and B are volcano and heatmaps obtained from differential expression analysis. C is a Venn diagram where the intersection of PRGs and DEG is taken. D is the boxplot of the expression of intersection genes in the COPD and control groups.

respectively. The diagnostic model constructed using the LR algorithm had a higher AUC than the other algorithms for the external dataset. Fig. 4B and C presents the ROC curves of the diagnostic model constructed based on these genes using the LR algorithm in the internal and external datasets. Fig. 5A and B and 5C-D respectively predicted the diagnostic performance of 14 genes in internal and external data sets.

3.3. Nomogram model construction and DCA analysis

In this study, 11 DRGs were used to construct a nomogram model and perform DCA. Fig. 6A and B shows the nomogram model and its calibration curve constructed in this study using 14DRGs. Analysis of the clinical impact curves showed that the nomogram model had relatively high diagnostic power (Fig. 6C). Finally, we verified the expression of DRGs in the two groups of the validation set and identified genes with significant differences (Fig. 6D–F). As can be seen from the figure, the expression levels of five genes (CASP5、CTSG, and MEFV) were significantly different between the two groups.

3.4. The immune landscape of DRGs

To explore the immune landscape of COPD, the CIBERSORT algorithm was used to calculate the infiltration abundance of 22 immune cells in all samples. Fig. 7A shows the proportion of immune cell infiltration richness of 22 immune cells in the COPD and control groups. After removing immune cells with zero abundance in 50% of the samples, Fig. 7B presents an abundance heatmap of the remaining 15 immune cells between the two groups. Fig. 7C shows a heat map of the correlation between immune cells, in which most cells showed a negative correlation. The results shown in Fig. 7D demonstrate a difference in the infiltration of 22 immune cells between the two groups. In both groups, there was a higher abundance of immune infiltration by T cells, resting CD4 memory cells, monocytes, M2 macrophages, and resting mast cells. The infiltration abundances of naïve B cells, CD8 + T cells, follicular helper T cells, gamma delta, M0 macrophages, resting dendritic cells, and activated dendritic cells significantly differed between the two groups ($p < 0.05$).

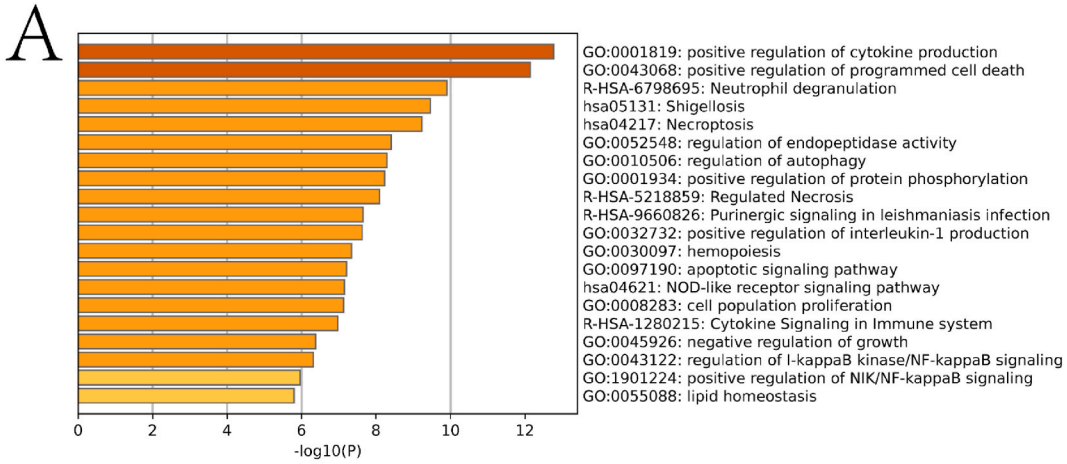

B

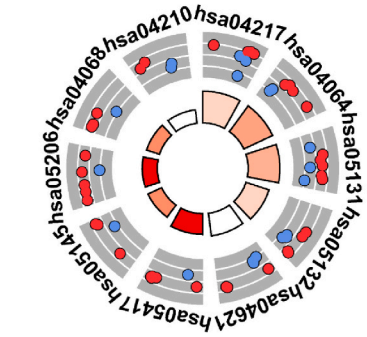

ID	Description
hsa04217	Necroptosis
hsa04064	NF−kappa B signaling pathway
hsa05131	Shigellosis
hsa05132	Salmonella infection
hsa04621	NOD−like receptor signaling pathway
hsa05417	Lipid and atherosclerosis
hsa05145	Toxoplasmosis
hsa05206	MicroRNAs in cancer
hsa04068	FoxO signaling pathway
hsa04210	Apoptosis

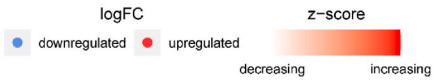

Fig. 3. Enrichment analysis of intersection genes. A and B are the results of KEGG enrichment analysis and metascape enrichment analysis of intersection genes, respectively.

Finally, we analyzed the correlation between DRGs and immune cells (Fig. 8A-N). All DRGs significantly correlated with at least two types of immune cell infiltration. In addition, we analyzed the DRGs and drug interaction network (Fig. S1 in the Supplementary Material), among which TUBB6, BCL2, and EGFR interacted with various compounds and are promising targets for related drugs.

3.5. Results of scRNA-seq data analysis

Here, we present a detailed analysis of the relevant subtypes of dendritic cell populations based on scRNA-seq data from COPD. Quality control, normalization, dimensionality reduction, clustering, and cell annotation were performed sequentially on raw scRNA-seq data. Final clustering yielded 24 cell populations (Fig. 9A). These cell populations were annotated as eight cell types (Fig. 9B and C), including NK cells, epithelial cells, T cells, monocytes, dendritic ceDC, B cells, smooth muscle cells, and macrophages. In this study, DEGs were identified in different cell populations. Fig. 9D presents a heat map of the expression of the top-ranked genes in different cell clusters for different cell populations. Fig. 7B shows that the abundance of infiltrating DCs differed significantly between the control and diseased groups. Therefore, GO and Metascape enrichment analyses were performed for the DEGs in the DC population (Fig. 9E and F). Most of the pathways involving the DEGs were confirmed to be related to the occurrence and development of COPD. The biological significance of these pathways is explored in detail in the Discussion section.

The results of the communication analysis of different cell types showed that macrophages, monocytes, and DC had numerous and strong interactions with other cell populations (Fig. 10A and B). Heat maps of the contributions of all signals to the efferent or afferent responses in different cell populations were also generated (Fig. 10C and D). The figure shows that the GALECTIN and GAS signaling pathways contributed more to afferent and efferent DCs. Therefore, we analyzed the expression of genes involved in both signaling

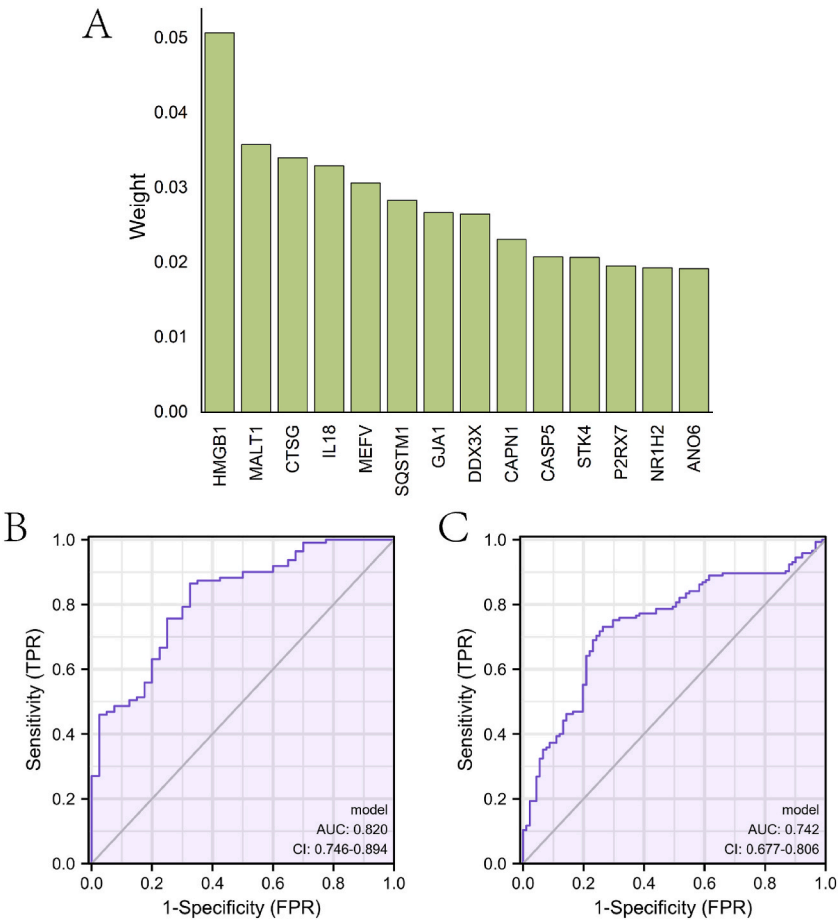

Fig. 4. The construction of diagnostic models. A is a bar graph of 14 genes with weights greater than the mean obtained using the RF algorithm and their corresponding weights. B and C are the ROC curves of the diagnostic model based on the LR algorithm using 14 genes in the internal and external datasets, respectively.

Table 1
The ROC curve information of the diagnostic models constructed by different machine learning algorithms in the internal dataset.

Algorithm	AUC	Sensitivity	Specificity
LR	0.82	0.87	0.68
RF	0.80	0.76	0.65
SVM	0.80	1	0.847
DNN	0.91	0.94	0.675

Table 2
ROC curve information of diagnostic models constructed by different machine learning algorithms in external datasets.

Algorithm	AUC	Sensitivity	Specificity
LR	0.74	0.73	0.74
RF	0.48	0.74	0.22
SVM	0.53	0.72	0.35
DNN	0.51	0.56	0.47

pathways in different cell types (Fig. 10E and F). PTPRC and CD44 are highly expressed in most cell populations via the GALECTIN pathway. LGAL59 and HAVCR2 were expressed at low levels in most cell populations. GAS6 and AXL are highly expressed in a few cell populations in the GAS pathway. MERTK and TYRO3 were expressed at low levels in all cell populations. We also showed network diagrams of the interactions between different cell populations under GALECTIN and GAS signaling (Fig. 10G and H).

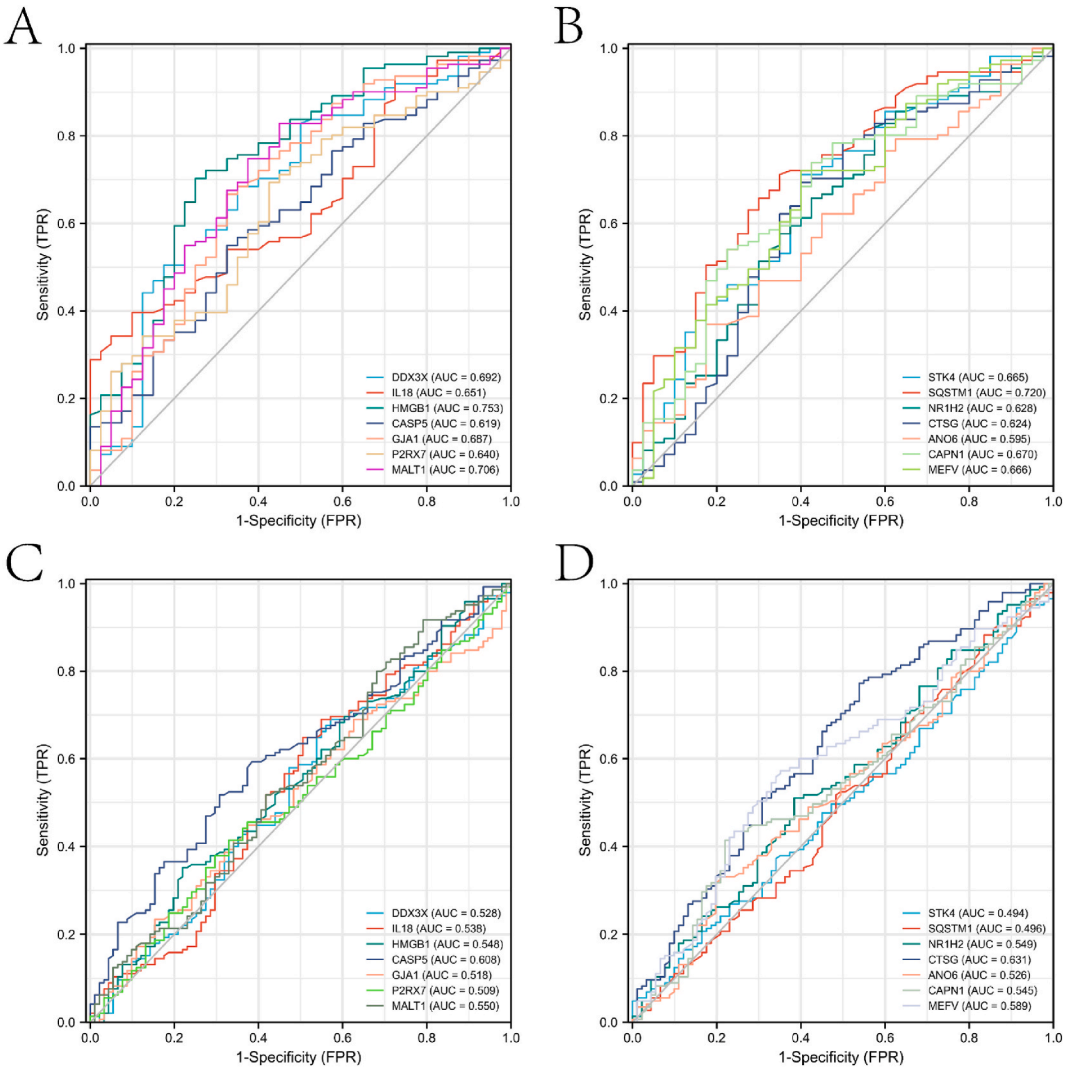

Fig. 5. Validation of diagnostic performance of 14 genes in internal and external datasets. A is the ROC curve of the top seven genes in the internal dataset. B is the ROC curve of the latter seven genes in the internal dataset. C is the ROC curve of the top seven genes in the external dataset. D is the ROC curve of the latter seven genes in the external dataset.

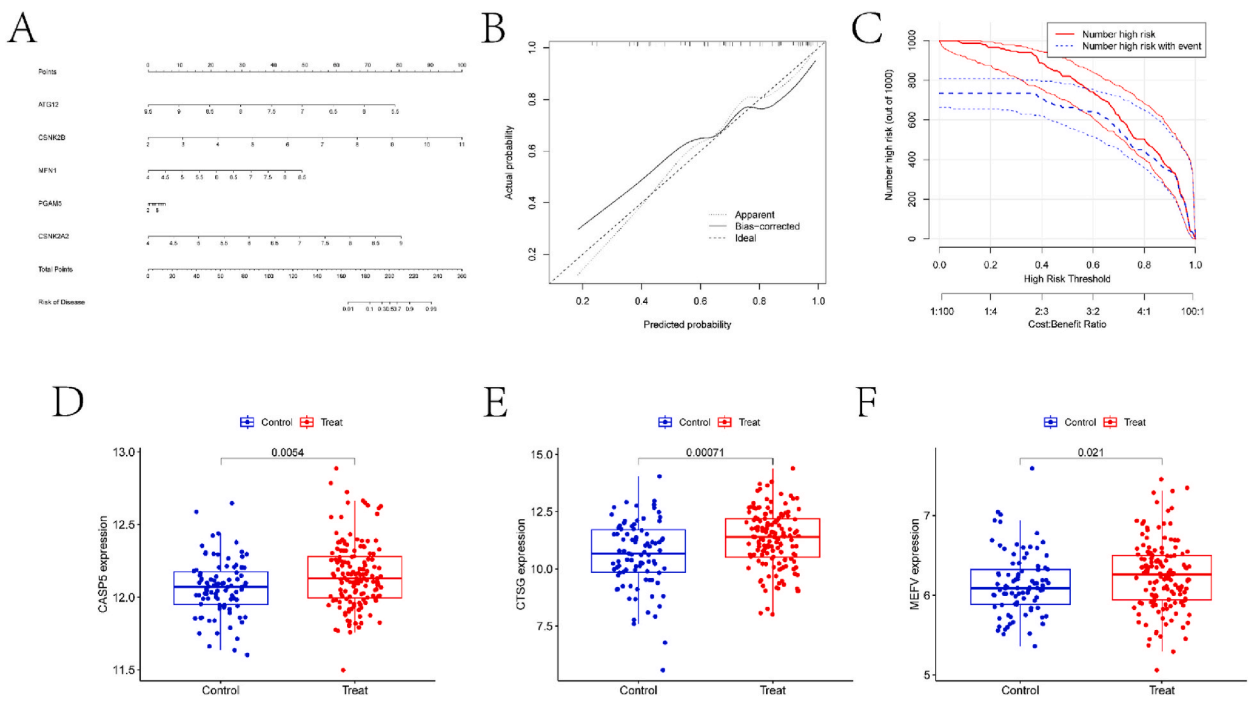

Fig. 6. Correlation analysis of diagnostic genes. A is the nomogram model for the diagnostic gene. B is the calibration curve of nomogram model. C. The clinical impact curve showed that the nomogram model had a high diagnostic ability. D-F is a boxplot of three genes (CASP5, CTSG, and MEFV) with significant differences in expression between the disease and control groups.

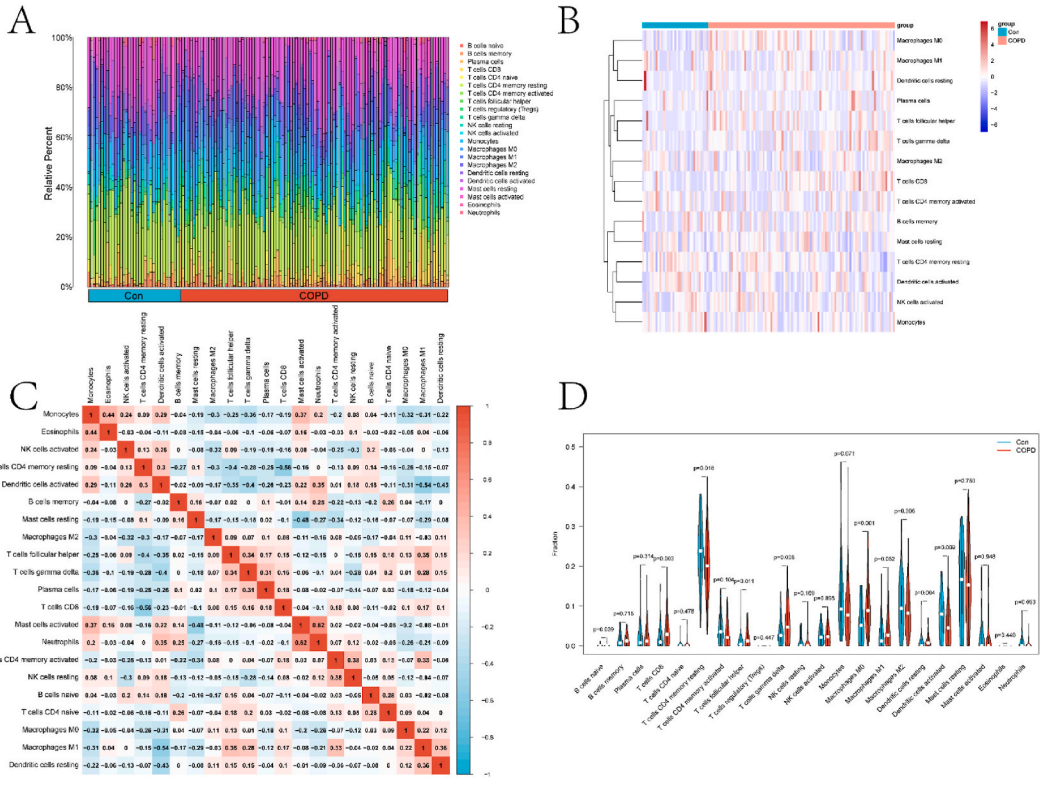

Fig. 7. The immune landscape of COPD. A is the proportion of immune cells obtained from CIBERSORT analysis of COPD and control groups. B is a heatmap of the abundance of immune infiltrates in the COPD and control groups. C is the immune cell correlation heatmap. D is the boxplot of the difference in the abundance of immune cell infiltration between COPD and control groups.

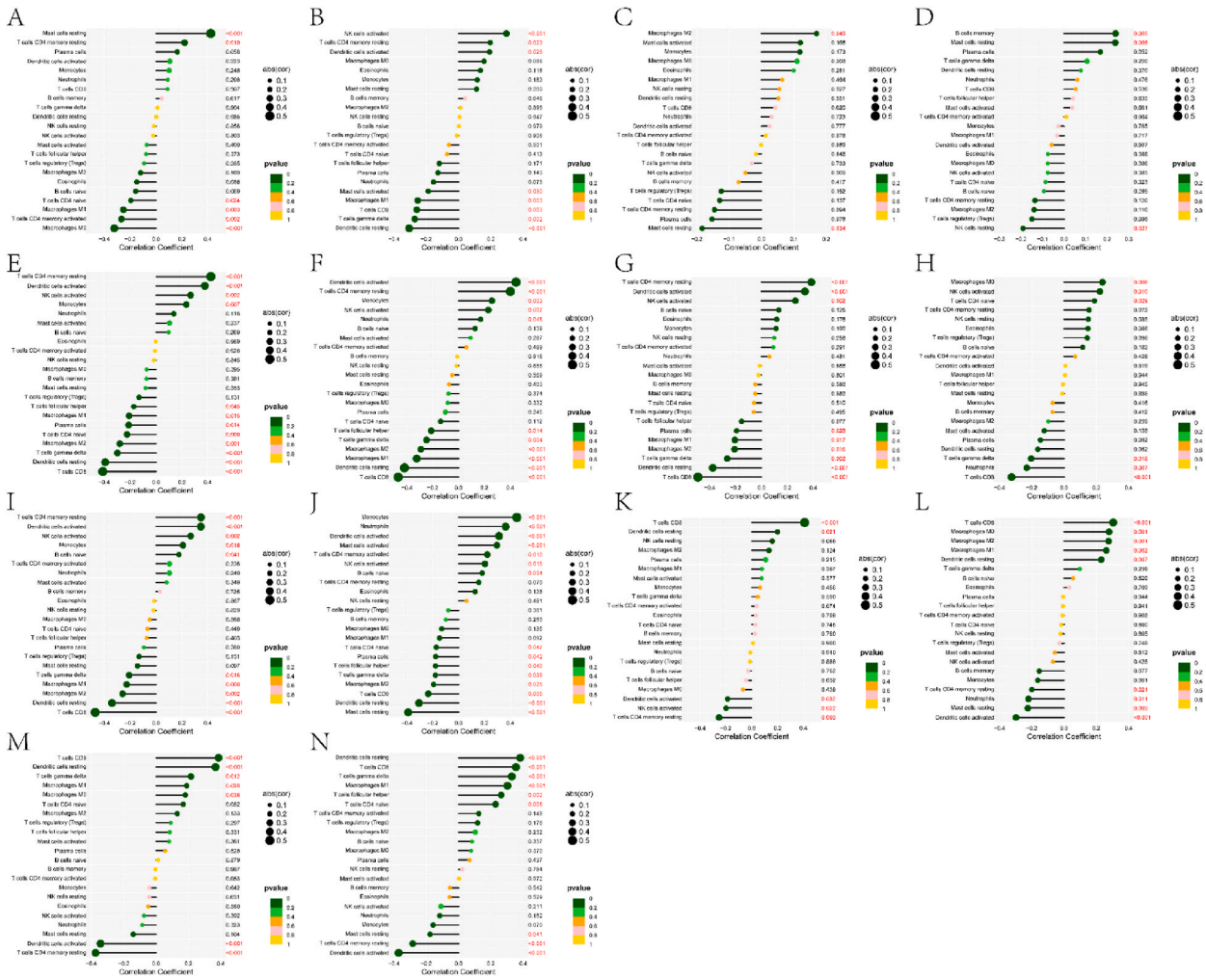

Fig. 8. Lollipop plot obtained from correlation analysis of 14 DRGs and immune cells. A-N are lollipop plots of the associations of ANO6, CAPN1, CASP5, CTSG, DDX3X, GJA1, HMGB1, IL18, MALT1, MEFV, NR1H2, P2RX7, SQSTM1 and STK4 with immune cells, respectively.

4. Discussion

The primary objective of this study was to elucidate the role of apoptosis-related genes in diagnosing COPD using various machine-learning methods. Notably, deep neural networks and logistic regression methods demonstrated outstanding classification accuracy in internal and external test sets, underscoring their potential clinical relevance. Our initial step involved rigorous preprocessing, encompassing batch effect removal and dataset integration to enhance the robustness of our analysis. Identifying apoptosis-related Differentially Expressed Genes (PDEGs) further elucidates the molecular landscape associated with COPD. Enrichment analyses using KEGG and Metascape highlighted the pathways closely linked to the development of COPD. Lu et al. showed that necroptotic signaling promotes inflammation in COPD [20]. Previous studies have shown that the innate immune response of the lungs to lipopolysaccharides (LPS) is closely associated with cellular inflammation. Bozinovski et al. showed that LPS inhibits the NF-kappa B signaling pathway [21]. In addition, Wang et al. found that aerobic exercise alleviates apoptosis in mice with COPD [22]. A retrospective study by Racanelli et al. showed that autophagy-related pathways play essential roles in the development of COPD [23]. Miller et al. showed that clonal hematopoiesis is significantly correlated with COPD [24]. Lodge et al. found that hypoxia increases the possibility of neutrophil-mediated endothelial damage in COPD [25].

To explore the diagnostic significance of PDEGs in COPD, we utilized the RF algorithm to assess the importance of each PDEG in the diagnosis and ranked them based on their importance. Specifically, 14 genes (ANO6, CAPN1, CASP5, CTSG, DDX3X, GJA1, HMGB1, IL18, MALT1, MEFV, NR1H2, P2RX7, SQSTM1, and STK4) with weights greater than the mean were retained to construct the diagnostic model. Receiver operating characteristic (ROC) curves were plotted for each gene. Several genes are associated with the occurrence and development of COPD. The pathogenesis of COPD is complex and mainly related to oxidative stress, overexpression, or activation of inflammatory factors and signaling pathways. In patients with COPD, macrophages and neutrophils enter the airway and

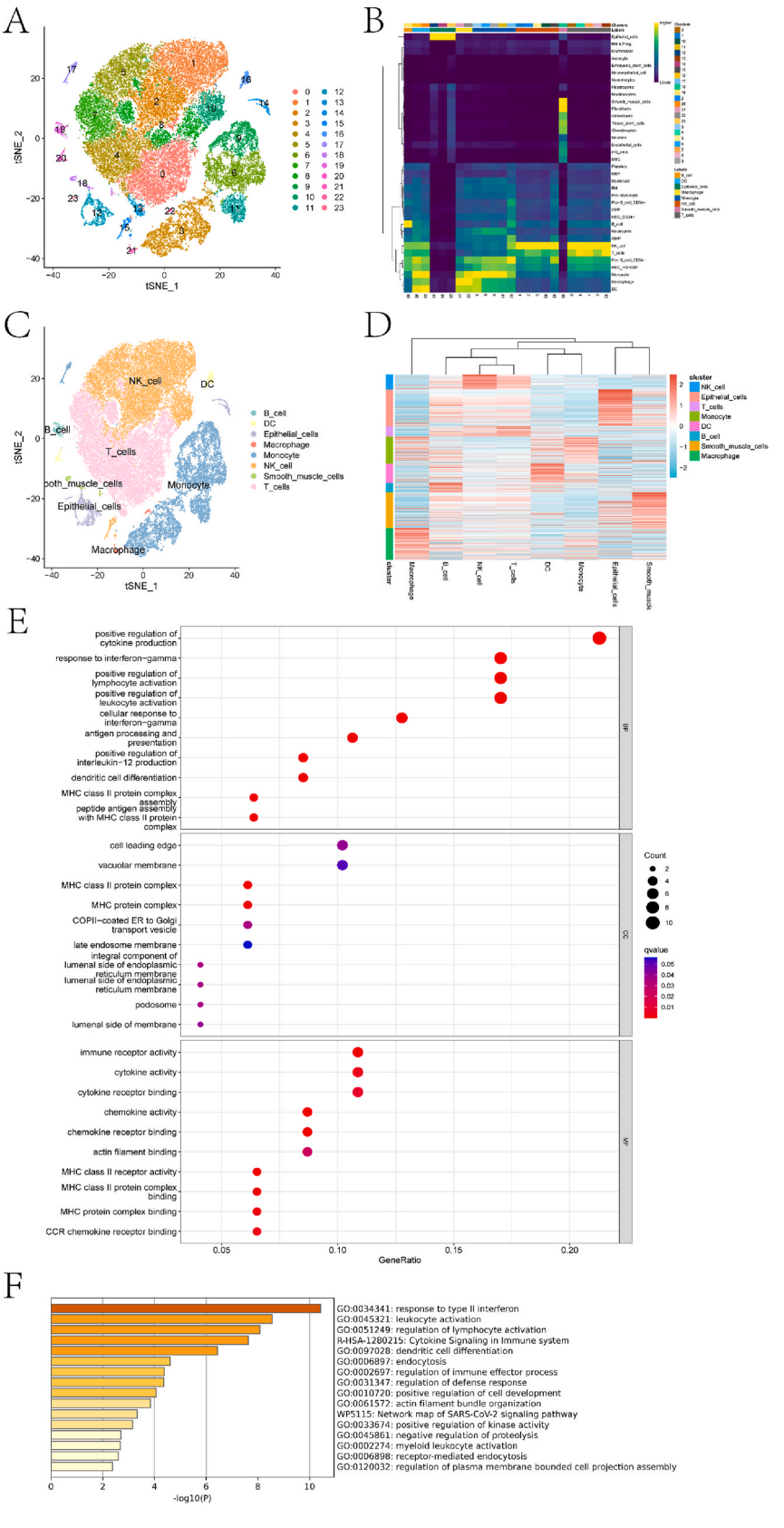

(caption on next page)

Fig. 9. Cell clustering and annotation results. A is the visualization of cell clustering results based on tsne. B is a heatmap based on the singleR package performing a score on the possible cell types to which the cell population belongs. C is the visualization of cell annotation results based on tsne. D is the expression heatmap of DEGs between different types of cell populations. E-F is the bubble plot and bar plot of GO and Metascape enrichment analyses performed on DEGs of the DC cell population, respectively.

upregulate chemokines, releasing large amounts of inflammatory factors that contribute to disease development [26]. CTSG (cathepsin G) may mediate tissue damage at sites of neutrophil-dominated inflammation [27]. Lung tissue destruction by proteinase 3 and cathepsin G-mediated elastin degradation is also elevated in COPD [28]. HMGB1 can promote extracellular DNA-induced activation of AIM2 inflammatory vesicles via AGER/RAGE [29]. HMGB1 also appears to regulate the adhesion and migration of neutrophils, similar to AGER/RAGE and ITGAM. Studies have confirmed that HMGB1 is involved in airway inflammatory processes and that its aberrant expression is associated with inflammation in COPD [30]. NLRP3 is associated with neutrophil migration and promotes interleukin-18 (IL-18) production. Guo et al. showed that NLRP3 is a potential therapeutic target for COPD [31]. MEFV is an autophagy receptor that degrades several inflammatory vesicle components (CASP1, NLRP1, and NLRP3) and prevents excessive IL1B and IL18-mediated inflammation [32–34]. The hepatic X receptors LXRA and LXRB (NR1H2) form a subfamily of the nuclear receptor superfamily and are key regulators of macrophage function, controlling the transcriptional programs involved in lipid homeostasis and inflammation. Dai et al. demonstrated that genetic polymorphisms in P2RX7 are significantly associated with altered COPD risk [35]. The literature above confirms the biological relevance of the proposed model. These findings contribute to a better understanding of the complex molecular mechanisms underlying COPD pathogenesis.

Exploring the differences in the abundance of immune cell infiltration between COPD and control groups is helpful for evaluating the therapeutic effects of COPD and related drug development. As shown in Fig. 7D, the infiltrating abundance of various immune cells significantly differed between the COPD and control groups. Polverino et al. reviewed the adaptive immune response in COPD and summarized the protective activity of B cells during acute exacerbations of COPD by promoting the adaptive immune response [36]. Qin et al. systematically reviewed the function and role of CD4 + helper T lymphocytes in chronic obstructive pulmonary disease, providing a new approach to guide the treatment of COPD [37]. CD8 (+) T cells are overrepresented in the lungs of COPD patients and are inversely correlated with lung function. Kemeny et al. showed that CD8 (+) T cells were overrepresented in the lungs of COPD patients and negatively associated with lung function [38]. The results of a miRNA-mRNA network analysis for COPD showed that the characteristics of the miRNA-mRNA network play an essential role in macrophage polarization [39]. Naessens et al. showed that conventional lung dendritic cells could coordinate lymphomagenesis in patients with COPD [40]. We analyzed the network of diagnosis-related genes associated with multiple compounds (Fig. S1). For example, epigallocatechin gallate has antioxidant and anti-inflammatory properties and can be used as a therapeutic agent for COPD [41]. Vollenweider et al. found that antibiotics (antibiotics) exacerbated COPD [42]. Nebulized fentanyl can be used to treat refractory dyspnea in patients with COPD with major complications and comorbidities [43]. This study further substantiated the significant differences in the cellular infiltration abundance between the two groups, emphasizing the biological significance of these cells.

To explore the expression of the identified diagnostic genes in different cell populations from a single-cell perspective, we analyzed scRNA-seq data from COPD patients. Specifically, a comprehensive analysis identified eight distinct cell populations, with particular emphasis on dendritic cells (DC), showing significant differences in infiltration abundance between the two groups. Further exploration of the pathways associated with the DEGs in DC provided additional evidence for their relevance to the progression of COPD. Marques et al. found that increased circulating platelets and mononuclear leukocytes expressing CXCR6 in patients with COPD may be markers of systemic inflammation [44]. Delayed rectifier K channels are likely overexpressed or overactivated in T lymphocytes isolated from patients with COPD, which would contribute to the development or progression of COPD [45]. Pulmonary macrophages are critical immune effector cells involved in COPD [46]. The activity of the ubiquitin-proteasome system has been linked to cellular events occurring in respiration and peripheral muscles of patients with COPD [47].

Finally, cell communication analysis revealed a close association of the galactolectin and GAS signaling pathways with DC, highlighting their potential as key players in the pathogenesis of COPD. We further explored the gene expression in both pathways in different cell populations. Some genes (LGALS9, PTPRC, HAVCR2, CD44A, GAS6, and AXL) were highly expressed in the DC. Maghsoudloo identified LGALS9 as a biomarker of COPD using a co-expression network and drug-target interaction analysis [48]. In addition, GAS6 and AXL are associated with the development of COPD [49,50].

We used a variety of bioinformatic analyses and machine learning methods to reveal the intricate interplay between genes associated with pyrodeath in COPD diagnosis. The identified diagnostic models and key pathways provide valuable insights for future research and potential clinical applications for COPD management.

5. Conclusion

Our study delved into the intricate landscape of apoptosis-related genes in COPD, revealing potential diagnostic biomarkers and elucidating their underlying mechanisms. Using machine learning algorithms, we identified 14 diagnostic genes with significant predictive accuracy through logistic regression. These genes, including ANO6, CAPN1, and CASP5, have been linked to COPD pathogenesis, affirming the biological relevance of our diagnostic model. Furthermore, our exploration of immune cell infiltration revealed substantial differences in abundance between the COPD and control groups, highlighting the complex interplay between various immune cells in the disease. Notably, dendritic cells have emerged as key participants, with single-cell RNA sequencing data indicating their unique roles in communication patterns and potential involvement in COPD progression.

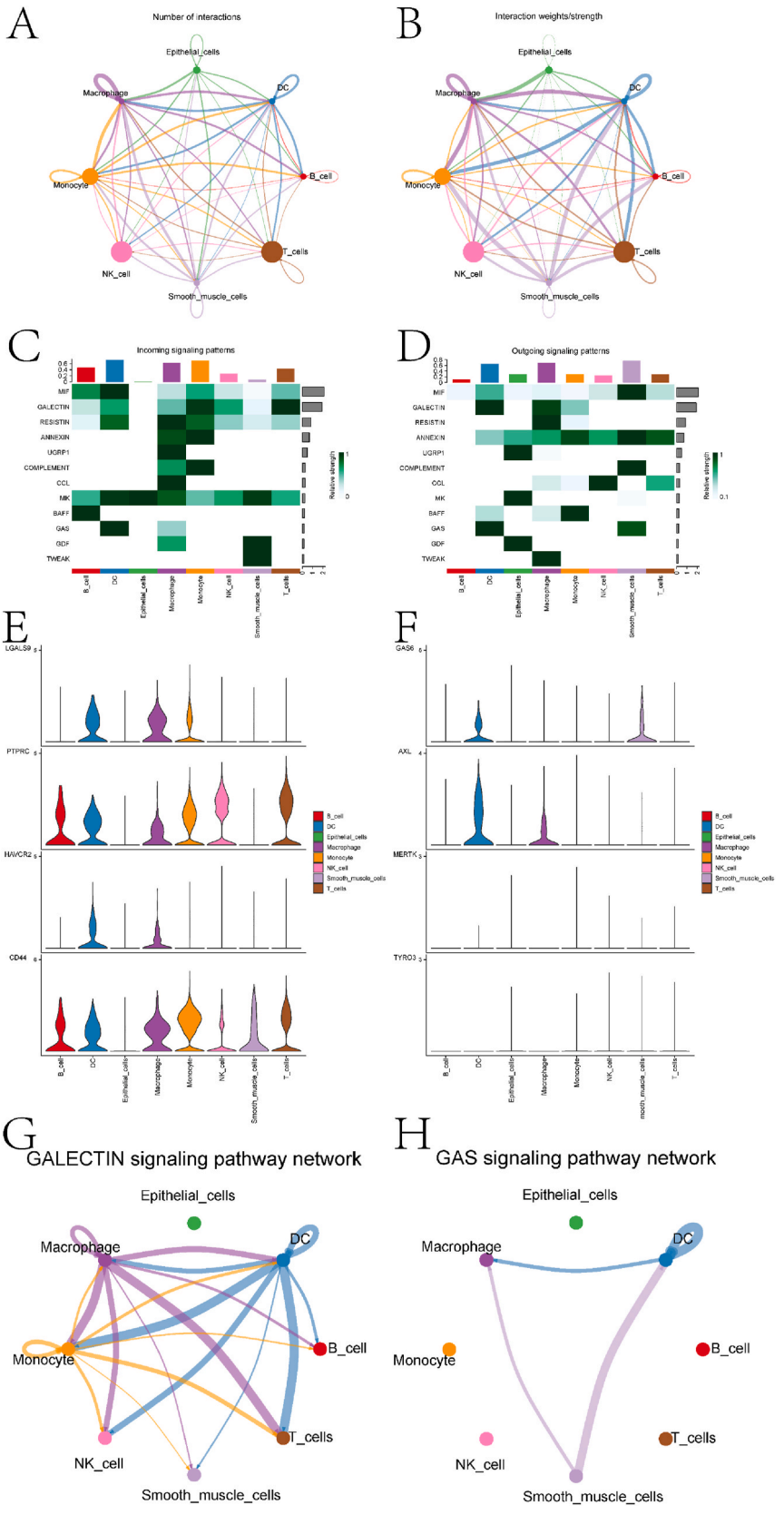

(caption on next page)

Fig. 10. Results of cell-to-cell communication analysis. A and B show the number and strength of interactions between various types of cells, respectively. C and D show the contributions of all signals to efferent or afferent responses of different cell populations, respectively. E and F show the expression heatmaps in each cell population of genes included in the two signaling pathways, GALECTIN and GAS, that contribute most to the afferent and efferent processes of DC cells, respectively. G and H show the interaction network diagram between GALECTIN and GAS signaling pathways in various types of cells, respectively.

Future research should focus on subtype analysis of COPD, dissecting the subtle differences in diagnosis, immunity, and drug sensitivity among different subgroups. The communication patterns of dendritic cells revealed multifaceted pathways associated with COPD, offering intriguing avenues for further exploration and targeted therapies. Our study contributes to a nuanced understanding of COPD and lays the foundation for future research and potential clinical applications.

Ethics approval and consent to participate

Not applicable.

Consent for publication

Not applicable.

Data availability statement

The COPD samples used in this paper are from GEO database (https://www.ncbi.nlm.nih.gov/geo/). GSE76925 data sets can be found at https://www.ncbi.nlm.nih.gov/geo/query/acc.cgi?acc=GSE76925. GSE47460 data sets can be found at https://www.ncbi.nlm.nih.gov/geo/query/acc.cgi?acc=GSE47460. GSE227691 data sets can be found at https://www.ncbi.nlm.nih.gov/geo/query/acc.cgi?acc=GSE227691.

Funding

The study was supported by Zhejiang Basic Public Welfare Research Program (LGF22H070001).

Ethics approval and consent to participate

Not applicable.

CRediT authorship contribution statement

Huiyan Zheng: Writing – review & editing, Writing – original draft, Methodology, Formal analysis, Data curation, Conceptualization. **Guifeng Wang:** Formal analysis, Data curation. **Yunlai Wang:** Formal analysis, Data curation. **Qixian Wang:** Formal analysis, Data curation. **Ting Sun:** Writing – review & editing, Supervision, Formal analysis.

Declaration of competing interest

The authors declare that they have no known competing financial interests or personal relationships that could have appeared to influence the work reported in this paper.

Acknowledgements

Not applicable.

Appendix A. Supplementary data

Supplementary data to this article can be found online at https://doi.org/10.1016/j.heliyon.2024.e27808.

References

[1] S. Sun, Y. Shen, J. Wang, J. Li, J. Cao, J. Zhang, Identification and validation of autophagy-related genes in chronic obstructive pulmonary disease, Int. J. Chronic Obstr. Pulm. Dis. 16 (2021) 67–78.

[2] Z. Lin, Y. Xu, L. Guan, L. Qin, J. Ding, Q. Zhang, L. Zhou, Seven ferroptosis-specific expressed genes are considered as potential biomarkers for the diagnosis and treatment of cigarette smoke-induced chronic obstructive pulmonary disease, Ann. Transl. Med. 10 (2022) 331.

[3] Y. Zhang, R. Xia, M. Lv, Z. Li, L. Jin, X. Chen, Y. Han, C. Shi, Y. Jiang, S. Jin, Machine-learning algorithm-based prediction of diagnostic gene biomarkers related to immune infiltration in patients with chronic obstructive pulmonary disease, Front. Immunol. 13 (2022) 740513.
[4] Q. Guan, Y. Tian, Z. Zhang, L. Zhang, P. Zhao, J. Li, Identification of potential key genes in the pathogenesis of chronic obstructive pulmonary disease through bioinformatics analysis, Front. Genet. 12 (2021) 754569.
[5] H. Han, L. Hao, Revealing lncRNA biomarkers related to chronic obstructive pulmonary disease based on bioinformatics, Int. J. Chronic Obstr. Pulm. Dis. 17 (2022) 2487–2515.
[6] Y. Li, B. Li, Y. Liu, H. Wang, M. He, Y. Liu, Y. Sun, W. Meng, Porphyromonas gingivalis lipopolysaccharide affects oral epithelial connections via pyroptosis, Journal of dental sciences 16 (2021) 1255–1263.
[7] L. Wang, X. Qin, J. Liang, P. Ge, Induction of pyroptosis: a promising strategy for cancer treatment, Front. Oncol. 11 (2021) 635774.
[8] R. Karki, T.D. Kanneganti, Diverging inflammasome signals in tumorigenesis and potential targeting, Nat. Rev. Cancer 19 (2019) 197–214.
[9] Y. Wang, W. Gao, X. Shi, J. Ding, W. Liu, H. He, K. Wang, F. Shao, Chemotherapy drugs induce pyroptosis through caspase-3 cleavage of a gasdermin, Nature 547 (2017) 99–103.
[10] L. Wang, Q. Chen, Q. Yu, J. Xiao, H. Zhao, TREM-1 aggravates chronic obstructive pulmonary disease development via activation NLRP3 inflammasome-mediated pyroptosis, Inflamm. Res. : official journal of the European Histamine Research Society 70 (2021) 971–980 [et al.].
[11] C. Zhang, W. Zhu, Q. Meng, N. Lian, J. Wu, B. Liu, H. Wang, X. Wang, S. Gu, J. Wen, et al., Halotherapy relieves chronic obstructive pulmonary disease by alleviating NLRP3 inflammasome-mediated pyroptosis, Ann. Transl. Med. 10 (2022) 1279.
[12] M.Y. Zhang, Y.X. Jiang, Y.C. Yang, J.Y. Liu, C. Huo, X.L. Ji, Y.Q. Qu, Cigarette smoke extract induces pyroptosis in human bronchial epithelial cells through the ROS/NLRP3/caspase-1 pathway, Life Sci. 269 (2021) 119090.
[13] G.K. Smyth, Linear models and empirical bayes methods for assessing differential expression in microarray experiments, in: Statistical Applications in Genetics and Molecular Biology, vol. 3, Article3, 2004.
[14] G. Yu, L.G. Wang, Y. Han, Q.Y. He, clusterProfiler: an R package for comparing biological themes among gene clusters, OMICS A J. Integr. Biol. 16 (2012) 284–287.
[15] L. Buitinck, G. Louppe, M. Blondel, F. Pedregosa, A. Mueller, O. Grisel, V. Niculae, P. Prettenhofer, A. Gramfort, J. Grobler, et al., API Design for Machine Learning Software: Experiences from the Scikit-Learn Project, 2013 **abs/1309.0238**.
[16] A.M. Newman, C.L. Liu, M.R. Green, A.J. Gentles, W. Feng, Y. Xu, C.D. Hoang, M. Diehn, A.A. Alizadeh, Robust enumeration of cell subsets from tissue expression profiles, Nat. Methods 12 (2015) 453–457.
[17] T. Stuart, A. Butler, P. Hoffman, C. Hafemeister, E. Papalexi, W.M. Mauck 3rd, Y. Hao, M. Stoeckius, P. Smibert, R. Satija, Comprehensive integration of single-cell data, Cell 177 (2019) 1888–1902.e1821.
[18] D. Aran, A.P. Looney, L. Liu, E. Wu, V. Fong, A. Hsu, S. Chak, R.P. Naikawadi, P.J. Wolters, A.R. Abate, et al., Reference-based analysis of lung single-cell sequencing reveals a transitional profibrotic macrophage, Nat. Immunol. 20 (2019) 163–172.
[19] S. Jin, C.F. Guerrero-Juarez, L. Zhang, I. Chang, R. Ramos, C.H. Kuan, P. Myung, M.V. Plikus, Q. Nie, Inference and analysis of cell-cell communication using CellChat, Nat. Commun. 12 (2021) 1088.
[20] Z. Lu, H.P. Van Eeckhoutte, G. Liu, P.M. Nair, B. Jones, C.M. Gillis, B.C. Nalkurthi, F. Verhamme, T. Buyle-Huybrecht, P. Vandenabeele, et al., Necroptosis signaling promotes inflammation, airway remodeling, and emphysema in chronic obstructive pulmonary disease, Am. J. Respir. Crit. Care Med. 204 (2021) 667–681.
[21] S. Bozinovski, J.E. Jones, R. Vlahos, J.A. Hamilton, G.P. Anderson, Granulocyte/macrophage-colony-stimulating factor (GM-CSF) regulates lung innate immunity to lipopolysaccharide through Akt/Erk activation of NFkappa B and AP-1 in vivo, J. Biol. Chem. 277 (2002) 42808–42814.
[22] X. Wang, Z. Wang, D. Tang, Aerobic exercise alleviates inflammation, oxidative stress, and apoptosis in mice with chronic obstructive pulmonary disease, Int. J. Chronic Obstr. Pulm. Dis. 16 (2021) 1369–1379.
[23] A.C. Racanelli, S.A. Kikkers, A.M.K. Choi, S.M. Cloonan, Autophagy and inflammation in chronic respiratory disease, Autophagy 14 (2018) 221–232.
[24] P.G. Miller, D. Qiao, J. Rojas-Quintero, M.C. Honigberg, A.S. Sperling, C.J. Gibson, A.G. Bick, A. Niroula, M.E. McConkey, B. Sandoval, et al., Association of clonal hematopoiesis with chronic obstructive pulmonary disease, Blood 139 (2022) 357–368.
[25] K.M. Lodge, A. Vassallo, B. Liu, M. Long, Z. Tong, P.R. Newby, D. Agha-Jaffar, K. Paschalaki, C.E. Green, K.B.R. Belchamber, et al., Hypoxia increases the potential for neutrophil-mediated endothelial damage in chronic obstructive pulmonary disease, Am. J. Respir. Crit. Care Med. 205 (2022) 903–916.
[26] P.S. Hiemstra, S. van Wetering, J. Stolk, Neutrophil serine proteinases and defensins in chronic obstructive pulmonary disease: effects on pulmonary epithelium, Eur. Respir. J. 12 (1998) 1200–1208.
[27] J.T. Benjamin, E.J. Plosa, J.M. Sucre, R. van der Meer, S. Dave, S. Gutor, D.S. Nichols, P.M. Gulleman, C.S. Jetter, W. Han, et al., Neutrophilic inflammation during lung development disrupts elastin assembly and predisposes adult mice to COPD, J. Clin. Invest. (2021) 131.
[28] N.S. Gudmann, T. Manon-Jensen, J.M.B. Sand, C. Diefenbach, S. Sun, A. Danielsen, M.A. Karsdal, D.J. Leeming, Lung tissue destruction by proteinase 3 and cathepsin G mediated elastin degradation is elevated in chronic obstructive pulmonary disease, Biochem. Biophys. Res. Commun. 503 (2018) 1284–1290.
[29] L. Liu, M. Yang, R. Kang, Y. Dai, Y. Yu, F. Gao, H. Wang, X. Sun, X. Li, J. Li, et al., HMGB1-DNA complex-induced autophagy limits AIM2 inflammasome activation through RAGE, Biochem. Biophys. Res. Commun. 450 (2014) 851–856.
[30] L. Lin, J. Li, Q. Song, W. Cheng, P. Chen, The role of HMGB1/RAGE/TLR4 signaling pathways in cigarette smoke-induced inflammation in chronic obstructive pulmonary disease, Immunity, inflammation and disease 10 (2022) e711.
[31] P. Guo, R. Li, T.H. Piao, C.L. Wang, X.L. Wu, H.Y. Cai, Pathological mechanism and targeted drugs of COPD, Int. J. Chronic Obstr. Pulm. Dis. 17 (2022) 1565–1575.
[32] J.J. Chae, G. Wood, S.L. Masters, K. Richard, G. Park, B.J. Smith, D.L. Kastner, The B30.2 domain of pyrin, the familial Mediterranean fever protein, interacts directly with caspase-1 to modulate IL-1beta production, Proc. Natl. Acad. Sci. U.S.A. 103 (2006) 9982–9987.
[33] S. Papin, S. Cuenin, L. Agostini, F. Martinon, S. Werner, H.D. Beer, C. Grütter, M. Grütter, J. Tschopp, The SPRY domain of Pyrin, mutated in familial Mediterranean fever patients, interacts with inflammasome components and inhibits proIL-1beta processing, Cell Death Differ. 14 (2007) 1457–1466.
[34] T. Kimura, A. Jain, S.W. Choi, M.A. Mandell, K. Schroder, T. Johansen, V. Deretic, TRIM-mediated precision autophagy targets cytoplasmic regulators of innate immunity, J. Cell Biol. 210 (2015) 973–989.
[35] Y. Dai, Z. Zhang, L. Xu, Y. Shang, R. Lu, J. Chen, Genetic polymorphisms of IL17A, TLR4 and P2RX7 and associations with the risk of chronic obstructive pulmonary disease, Mutat. Res. Genet. Toxicol. Environ. Mutagen 829–830 (2018) 1–5.
[36] F. Polverino, L.J. Seys, K.R. Bracke, C.A. Owen, B cells in chronic obstructive pulmonary disease: moving to center stage, Am. J. Physiol. Lung Cell Mol. Physiol. 311 (2016) L687–l695.
[37] K. Qin, B. Xu, M. Pang, H. Wang, B. Yu, The functions of CD4 T-helper lymphocytes in chronic obstructive pulmonary disease, Acta Biochim. Biophys. Sin. 54 (2022) 173–178.
[38] D.M. Kemeny, B. Vyas, M. Vukmanovic-Stejic, M.J. Thomas, A. Noble, L.C. Loh, B.J. O'Connor, CD8(+) T cell subsets and chronic obstructive pulmonary disease, Am. J. Respir. Crit. Care Med. 160 (1999) S33–S37.
[39] W. Shen, S. Wang, R. Wang, Y. Zhang, H. Tian, X. Yang, W. Wei, Analysis of the polarization states of the alveolar macrophages in chronic obstructive pulmonary disease samples based on miRNA-mRNA network signatures, Ann. Transl. Med. 9 (2021) 1333.
[40] T. Naessens, Y. Morias, E. Hamrud, U. Gehrmann, R. Budida, J. Mattsson, T. Baker, G. Skogberg, E. Israelsson, K. Thörn, et al., Human lung conventional dendritic cells orchestrate lymphoid neogenesis during chronic obstructive pulmonary disease, Am. J. Respir. Crit. Care Med. 202 (2020) 535–548.
[41] S.P. Lakshmi, A.T. Reddy, L.D. Kodidhela, N.C. Varadacharyulu, Epigallocatechin gallate diminishes cigarette smoke-induced oxidative stress, lipid peroxidation, and inflammation in human bronchial epithelial cells, Life Sci. 259 (2020) 118260.
[42] D.J. Vollenweider, A. Frei, C.A. Steurer-Stey, J. Garcia-Aymerich, M.A. Puhan, Antibiotics for exacerbations of chronic obstructive pulmonary disease, Cochrane Database Syst. Rev. 10 (2018) Cd010257.

[43] L. Hildreth, D. Pett, E. Higgins, Nebulized fentanyl for refractory dyspnea secondary to chronic obstructive pulmonary disease (COPD): a case report, Respiratory medicine case reports 31 (2020) 101251.
[44] P. Marques, A. Collado, P. Escudero, C. Rius, C. González, E. Servera, L. Piqueras, M.J. Sanz, Cigarette smoke increases endothelial CXCL16-leukocyte CXCR6 adhesion in vitro and in vivo. Potential consequences in chronic obstructive pulmonary disease, Front. Immunol. 8 (2017) 1766.
[45] I. Kazama, T. Tamada, Lymphocyte Kv1.3-channels in the pathogenesis of chronic obstructive pulmonary disease: novel therapeutic implications of targeting the channels by commonly used drugs, Allergy Asthma Clin. Immunol. : official journal of the Canadian Society of Allergy and Clinical Immunology 12 (2016) 60.
[46] K. Akata, K. Yamasaki, F.S. Leitao Filho, C.X. Yang, H. Takiguchi, B. Sahin, B.A. Whalen, C.W.T. Yang, J.M. Leung, D.D. Sin, et al., Abundance of non-polarized lung macrophages with poor phagocytic function in chronic obstructive pulmonary disease (COPD), Biomedicines 8 (2020).
[47] R. Debigaré, C.H. Côté, F. Maltais, Ubiquitination and proteolysis in limb and respiratory muscles of patients with chronic obstructive pulmonary disease, Proc. Am. Thorac. Soc. 7 (2010) 84–90.
[48] M. Maghsoudloo, S. Azimzadeh Jamalkandi, A. Najafi, A. Masoudi-Nejad, Identification of biomarkers in common chronic lung diseases by co-expression networks and drug-target interactions analysis, Mol. Med. (Camb.) 26 (2020) 9.
[49] K.Y.F. Tsai, K.M. Hirschi Budge, S. Llavina, T. Davis, M. Long, A. Bennett, B. Sitton, J.A. Arroyo, P.R. Reynolds, RAGE and AXL expression following secondhand smoke (SHS) exposure in mice, Exp. Lung Res. 45 (2019) 297–309.
[50] S. Vasudevan, J.J. Vásquez, W. Chen, B. Aguilar-Rodriguez, E.C. Niemi, S. Zeng, W. Tamaki, M.C. Nakamura, M. Arjomandi, Lower PDL1, PDL2, and AXL expression on lung myeloid cells suggests inflammatory bias in smoking and chronic obstructive pulmonary disease, Am. J. Respir. Cell Mol. Biol. 63 (2020) 780–793.